Controlling Regular and Chaotic Dynamics in the Duffing-Ueda Oscillator

L A Aguirre and S A Billings

Department of Automatic Control and Systems Engineering
University of Sheffield
P.O. Box 600
Mappin Street
Sheffield S1 4DU
United Kingdom

Research Report No 477

May 1993

Controlling Regular and Chaotic Dynamics in the Duffing-Ueda Oscillator

LUIS A. AGUIRRE and S. A. BILLINGS

Abstract

This paper investigates the control of a forced nonlinear oscillator which is composed of a series-connected resonant circuit with a nonlinear inductor commonly known as Duffing's oscillator. Two control strategies are suggested. The first is primarily concerned with suppressing chaos by means of adding an external weak force to the input driving the oscillator. The second procedure uses a reference model to produce appropriate reference chaotic and nonchaotic signals for the oscillator to track. It is shown that this control scheme is effective in both regulating and tracking problems. Although it is possible to dispense with the reference model in many applications it is often highly desirable to obtain a model of the system. A practical and effective procedure for determining the model is therefore discussed. A discrete model of the oscillator, which had been previously obtained from the system with no *a priori* information, is used in several simulated examples provided to illustrate the main points of the paper.

1 Introduction

It is now an accepted fact that chaotic dynamics are far from being a rare phenomenon exhibited by a few pathological *ad hoc* models. On the contrary, chaos has been found in virtually all the branches of science in systems operating over wide ranges of conditions. In this respect, electrical circuits are no exception, see References [1, 2, 3, 4, 5, 6, 7, 8] for some examples.

Manuscript received on

The authors are with the Department of Automatic Control and Systems Engineering, University of Sheffield, P.O. Box 600, Mappin Street, Sheffield S1 4DU - UK. e-mail:aguirre@acse.sheffield.ac.uk

This work has been partially supported by CNPq (Brazil) under grant 200597/90-6 and SERC (UK) under grant GR/H 35286

One of the most peculiar features of a chaotic system is the sensitive dependence on initial conditions caused by local divergence of trajectories in the state-space along the 'directions' associated with positive Lyapunov exponents[1]. Consequently, it is impossible to make accurate long-term predictions of a system exhibiting chaotic dynamics.

In many situations, it is desirable that the system under investigation be predictable. Furthermore, the appearance of chaotic dynamics is sometimes associated with abnormal behavior [11, 12]. On the other hand, some authors have suggested that chaotic dynamics indicate a healthy state as opposed to the diseases which manifest as physiological periodic signals [13, 14].

Consequently, techniques for controlling nonlinear dynamics are required in order to provoke or suppress chaos or any other dynamical regime according to the particular need at hand. Unsurprisingly, a number of papers have been published recently regarding this matter. Some techniques were developed to bring a system which is in a chaotic state to some non-specified periodic behavior [15, 16, 17, 18, 19]. Other methods aim at stabilizing a chaotic system to a particular dynamical regime [12, 20, 21, 22]. Although it has been argued that these approaches are fairly general, the application of such methods to electrical oscillators has not received due attention.

The only exception seems to be the recent paper by Rajasekar and Lakshmanan [23] in which five of the aforementioned techniques were used to suppress chaos in the Bonhoeffer-van der Pol oscillator. The methods investigated were *adaptive control* (AC) [24, 25], *small parametric perturbation* (SPP), *addition of an external weak force* (AEWF) [16], *small parameter adjustment* (SPA) and *addition of noise* (AN) [26].

The AC method and related techniques assume that one may perturb a system parameter to perform the control [20]. In many practical situations, however, no such parameter is available, see Reference [12] for an example. The SPP method also presents this deficiency. In this respect the AEWF, SPA and AN methods are more appropriate. However, the AEWF and AN methods perform the control in open-loop (note that so does the SPP method). This, of course, assumes that the equations which describe the dynamics are known and that no unknown parameter perturbations occur.

[1] For an introduction to Lyapunov exponents see [9], and Reference [10] for a more detailed exposition on the subject.

Brown, Chua and Popp have recently shown that sensitive dependence on initial conditions is equivalent to sensitive dependence on parameters [27]. In other words, the basins of attraction are fractal in both the state and the parameter spaces. Thus if a certain system presents regular motions for a particular parameter value $\mu = \mu_o$, one cannot assume that the dynamics will still be qualitatively similar if the system is disturbed to $\mu = \mu_o + \delta$. It seems that this assumption has been made in [20] and in all the open-loop techniques. As a consequence, even if the equations which describe the dynamics of a potentially chaotic system which is to be controlled were known, because such a system exhibits sensitive dependence on the parameter values, the performance of open-loop schemes would be totally uncertain.

This paper investigates the control of the electrical oscillator which is modeled by the well known Duffing-Ueda equation. Two control schemes are suggested, namely, i) the addition of an external weak force operating in closed-loop, and ii) a model-based control scheme (MBCS).

Unlike most of the aforementioned methods, this paper does *not* assume a) that the model of the system is known[2], b) that a particular parameter is available for control, c) that only small adjustments are allowed, d) that local dynamics about a particular orbit do not vary much when small changes in a parameter take place, and e) that the system parameters are not subject to unknown disturbances.

Some of the advantages of the suggested control schemes are a) simplicity, b) robustness with respect to measurement noise and major parameter disturbances, c) the oscillator can be controlled at specific regular dynamical regimes and d) the oscillator dynamics can be constrained to lie on specific strange or non-strange attractors in the state space (for the MBCS only).

The paper is organized as follows. In §2 the nonlinear circuit and the respective differential equation are reviewed. In addition, a bifurcation diagram of the oscillator over a wide range of operating conditions is presented and briefly described. In §3 a simple procedure is proposed for suppressing chaos which is based on the addition of an external

[2]Although the MBCS uses a reference model, it will be argued that in many applications this model is not absolutely necessary. Moreover, it will also be indicated how such a model can be obtained directly from the system with no *a priori* knowledge, see §4.3.

weak force in closed-loop. Three simulated examples are provided which illustrate the suppression of chaos and also suggest that, in some cases, this technique can be used to stabilize the oscillator at period-K motions where K may be specified by the practitioner. Section 4 describes a model-based control scheme which can be used to drive the oscillator to specific dynamical regimes, regular or chaotic. Four simulated examples are provided which illustrate that this scheme is effective in regulating and tracking problems. Finally, the main points of the paper are summarized in §5.

2 The Duffing-Ueda Oscillator

Over the years, a few systems have become bench tests in the study of nonlinear oscillations. Two classical examples are the Duffing and van der Pol oscillators. Besides, several variants have also been suggested and investigated. This paper uses a version of Duffing's oscillator which has been studied by Ueda [28, 29, 30]. Hence this oscillator will be referred to as the Duffing-Ueda oscillator to distinguish it from other popular version, the Duffing-Holmes equation which is used to model mechanical vibrating systems [31].

Other versions of Duffing and van der Pol's electrical oscillators can be found in References [32, 33].

2.1 The circuit

Consider the circuit in Fig. 1. The equations for this circuit are [30]

$$\left.\begin{aligned} E\sin(\omega t) &= n\frac{d\phi}{dt} + Ri_r \\ Ri_r &= \frac{1}{C}\int i_c dt \\ i &= i_r + i_c \end{aligned}\right\} \tag{1}$$

where n is the number of turns of the inductor coil, and ϕ is the magnetic flux in the core. It is assumed that the saturation curve of the core can be expressed by [30]

$$i = a\Phi_n^3 \tag{2}$$

and that the effect of hysteresis is negligible. Define the dimensionless variable y as

$$y \doteq \frac{\phi}{\Phi_n} \tag{3}$$

where Φ_n is an appropriate base for the flux which satisfies the following relation

$$n\omega^2 C\Phi_n = a\Phi_n^3 \tag{4}$$

After some algebraic manipulations, the following well known Duffing-Ueda equation is obtained [30]

$$\ddot{y} + k\dot{y} + y^3 = u(t) \tag{5}$$

where

$$\left.\begin{aligned} k &= \tfrac{1}{\omega CR} \\ u(t) &= A\cos(\tau) \\ \tau &= \omega t - \tan^{-1} k \\ B &= \tfrac{E}{n\omega\Phi_n}\sqrt{1-k^2} \end{aligned}\right\} \tag{6}$$

Equation (5) has become a bench test for the study of nonlinear dynamics [28, 29, 30]. It has also been considered as a simple paradigm for chaotic dynamics in electrical science [34]. One of the main reasons for this is that in spite of being simple this model can produce a variety of dynamical regimes.

2.2 The dynamics

The dependence of the dynamics of a system upon a certain parameter, usually called the control parameter, is revealed by bifurcation diagrams. For a fixed value of the control parameter a cross section of the attractor can be obtained by appropriately sampling the system trajectories in state-space. This technique is called Poincaré sampling and the resulting cross section is a Poincaré section of the attractor. The computation of bifurcation diagrams and Poincaré sections is now a fairly standard procedure in the analysis of nonlinear systems and more details can be found elsewhere [34, 35].

Figure 2a shows the bifurcation diagram of the Duffing-Ueda oscillator with $k=0.1$, $\omega=1$ rad/s and $u(t)=A\cos(\omega t)$. This was obtained simulating equation (5) digitally using a fourth-order Runge-Kutta algorithm with an integration interval equal to $\pi/3000$ s. In the figure, the horizontal axis corresponds to the control parameter, A. As can be seen,

varying this parameter in the range $4.5 \leq A \leq 12$ drives the system into a number of different dynamical regimes.

Beginning at $A \approx 4.86$ the system undergoes a period doubling (flip) bifurcation. This happens again at $A \approx 5.41$ and characterizes the well known period doubling route to chaos [36]. Another similar cascade begins at $A \approx 9.67$ preceding a different chaotic regime. Two chaotic windows can be distinguished at approximately $5.55 \leq A \leq 5.82$ and $9.94 \leq A \leq 11.64$. At $A \approx 6.61$ the system undergoes a supercritical pitchfork bifurcation and at $A \approx 9.67$ it undergoes a subcritical pitchfork bifurcation. The bifurcation diagram begins and ends with period-one regimes and displays period-three dynamics for $5.82 \leq A \leq 9.67$.

Figure 2b shows a Poincaré section of the attractor obtained by sampling $y(t)$ at $t = j\pi$, $j = 0, 2, 4, \ldots$ and by plotting $y(t - T_s)$ against $y(t)$. In this figure $T_s = 200 \times \pi/3000$ s. This figure clearly reveals the fractal structure of the chaotic (strange) attractor obtained for this input.

3 Controlling the loss of chaos in closed-loop

The objective of the following procedure is to drive a system originally operating in a chaotic regime to a regular state by means of an *external* control action. This is an important point since some methods assume that a system parameter is available to perform the control [20], but, of course, this is not always so in practice [12].

3.1 The suggested control configuration

Braiman and Goldhirsch have shown that by adding a weak periodic perturbation to a system operating in a chaotic regime, such a system can be driven to regular periodic motions [16]. Kapitaniak has investigated the loss of chaos provoked by the addition of a random perturbation [26]. In these papers the model of the system was assumed to be known and no disturbances were allowed to take place.

In order not to make the same restrictive assumptions, it is necessary to perform the control in a closed-loop fashion. To achieve this consider the control configuration in Fig. 3.

The oscillator. The nonlinear oscillator is the circuit of Fig. 1 whose dynamics are governed by equation (5) which was simulated as before. It is assumed that the oscillator is originally operating in a chaotic steady-state regime. Moreover, equation (5) is not available to the controller.

The sensor. The sensor is composed of a *fixed-point counting algorithm* (FPCA) in conjunction with a *Poincaré-sampling device* (PSD). When the PSD is activated, a Poincaré section, **P**, of the attractor is produced at the output. The FPCA then determines the *number of fixed-points* (N_{fp}) in **P**. Further, the PSD is activated during N_a forcing periods at intervals of N_i forcing periods during which it remains inactive.

In practice a tolerance ϵ is defined such that all the points, p_i, of **P** satisfying

$$\| p_i - p_j \| < \epsilon \quad \forall\, i = j \tag{7}$$

are considered a single fixed point. It is noted that more than one norm may be used in equation (7) to quantify the distance between two points in **P**.

The controller. Based on N_{fp}, the controller verifies if the dynamics are chaotic and outputs a weak force computed according to a predefined law. If the system is in a chaotic state **P** will have N_a points. On the other hand, if the system is in a regular motion of period K then, no matter how long N_a might be, **P** will have K fixed-points. This is an extremely simple criterion which can be used to determine some of the topological properties of the attractor and ultimately verify if the oscillator is undergoing periodic or aperiodic motions.

The controller can be set to produce periodic or random outputs of small amplitude [16, 26]. If the objective is to suppress chaos, the controller increments the output amplitude until $N_{fp} < N_a$, which indicates that the output, $y(t)$, is periodic.

One of the advantages of this procedure is that a *desired number of fixed points* (D_{fp}) can be fixed as a set-point. In this case the controller will operate until $N_{fp} = D_{fp}$.

3.2 Simulation results

3.2.1 Simulation 1

In this simulation the control was performed in open-loop to illustrate some of the pitfalls of this approach. Assume that $u(t) = 11.5\cos(t)$. It is clear from Fig. 2a that the oscillator

exhibits chaotic dynamics when excited by this input. The objective is to drive the system to a non-chaotic regime.

In this example the control signal is $m(t) = A_c cos(\omega_c t)$ and $A_c \ll A$. It is noted that $m(t)$ is *external* to the system unlike many schemes which actuate on the system parameters.

According to the procedure outlined by Braiman and Goldhirsch, a Lyapunov table can be obtained for various values of A_c and ω_c. Any combination of these parameters for which the respective largest Lyapunov exponent, λ_1, is negative can be used to compose $m(t)$ and in this way suppress chaos [16]. Following this procedure the control signal $m(t) = 1.08cos(2.857142t)$ was applied to the oscillator in addition to the normal input and, as expected, the system was driven to a regular (period-seven) attractor with $\lambda_1 = -6.53 \times 10^{-2}$.

In a real application, however, the exact parameter values of the system will not be available in order to compute the Lyapunov table. Thus suppose that the actual value of k in equation (5) is 0.11 instead of 0.1 (which is already a fairly good approximation!). If the same control is applied to the system with $k = 0.11$, the oscillator will still be in a chaotic regime with an attracting set for which the largest Lyapunov exponent is $\lambda_1 = 1.81 \times 10^{-2}$. This illustrates the need for feedback in real control applications.

3.2.2 Simulation 2

In this simulation, the perturbed and unperturbed oscillators of simulation 1 were controlled in closed-loop in order to suppress chaos.

The following parameter values were used: K_p=0.05, ϵ=0.01, N_t=100 and N_a=30. As before, the oscillator was originally operating with $u(t) = 11.5cos(t)$ when the control was switched on and the control signal action was $m(t) = A_c cos(2.857142t)$.

A_c was initially set to zero and subsequently increased according to

$$A_c := A_c + K_p E \tag{8}$$

where $K_p \in \mathbb{R}$ is a constant gain and $E \in \mathbb{Z}$ is the error between D_{fp} and N_{fp}. If no specific periodicity is desired, D_{fp} could have any value such that $D_{fp} < N_a$, the controller

should be desactivated as soon as $N_{fp} < N_a$ regardless the value of E. A similar procedure was followed in Reference [17].

In the case of the unperturbed oscillator ($k = 0.1$), the output was drived to a regular (period-seven) orbit after four control cycles (note that each control cycle corresponds to $N_a + N_i$ input periods) with A_c=1.2. For the perturbed oscillator ($k = 0.11$), six control cycles were necessary to drive the output to a period-seven motion with A_c=1.6. As expected, both unperturbed and perturbed systems were operating in a non-chaotic motion after feedback control had been applied.

It is interesting to note that the controlled outputs are period-seven motions with respect to the input $u(t)$, that is the outputs were sampled at the same frequency of $u(t)$ in order to compose P. However, with respect to the total exciting signal $u(t)-m(t)$ the output is a period-one motion. It has been argued that in some situations stabilizing the system at high-period orbits might be advantageous [15].

3.2.3 Simulation 3

The objective in this simulation was not only to suppress chaos but also to drive the output to a period-eight motion.

The oscillator was originally set to operate with $u(t) = 5.6cos(t)$ which corresponds to the narrower chaotic window in Fig. 2a. In this case $\omega_c = 1$ rad/s and $D_{fp} = 8$ in addition to the parameter values used in the previous simulation.

The experiment was carried out for the original oscillator ($k = 0.1$) and for the perturbed oscillator ($k = 0.11$). Table 1 shows the main results.

Because of the disturbance in the system parameters, the control signal and also the dynamics of the controlled oscillators are different. Nevertheless, in both cases the controlled oscillators are driven to period-eight orbits.

Table 1. Dynamical regimes for the perturbed and unperturbed oscillators and respective control action $m(t) = A_c cos(2.857142t)$

	$k = 0.1$		$k = 0.11$	
Step	Dynamics	A_c	Dynamics	A_c
1	Chaos	0	Chaos	0
2	Chaos	-3.5×10^{-2}	Period-4	-3.5×10^{-2}
3	Period-12	-7.0×10^{-2}	Period-8	-1.5×10^{-2}
4	Period-4	-1.05×10^{-1}	Period-8	-1.5×10^{-2}
5	Period-8	-8.5×10^{-2}	Period-8	-1.5×10^{-2}
6	Period-8	-8.5×10^{-2}	Period-8	-1.5×10^{-2}

Figure 4 shows the sequence of Poincaré sections, P, corresponding to steps two to five in Table 1 for the unperturbed system.

It is noted that if the final control action of the perturbed system were applied to the original oscillator the output would still be chaotic. On the other hand, if the final control action of the unperturbed system were applied to the perturbed oscillator the output would display a period-four motion.

3.2.4 Remarks

The Poincaré section, P, can be obtained, as in Fig. 4, using the output at two different times, say $y(t)$ and $y(t - T_p)$, instead of using $y(t)$ and $\dot{y}(t)$ [37, 38]. In this example $T_p = 200 \times \pi/3000$ s.

The control strategy suggested above does not guarantee that a *specific* period-K orbit be finally attained because *any* period-K orbit will satisfy the requirement D_{fp}=K.

In the three simulations described above, the spectral power of $u(t)$ and of $u(t)+m(t)$ were virtually the same. This illustrates the well known fact that a very weak signal may be used to control a chaotic system. Moreover, this property has been described as a key feature of chaos which has a promising potential use in control applications [21].

The value of ω_c used in simulations 1 and 2 was chosen based on Lyapunov tables of the perturbed and unperturbed systems in order to illustrate that small perturbations in

the system parameters may lead to qualitatively different outputs and therefore justify the need for feedback. An interesting point to note is that in simulations 1 and 2 ω_c was close to the frequency of the third harmonic and in simulation 3 close to the fundamental frequency. Braiman and Goldhirsch have used a simple relation to show that the addition of a weak force reduces the value of the largest Lyapunov exponent and this result was independent of the frequency [16]. However, in other situations chaos was suppressed when the weak force was added at some resonant frequency [39].

The value of the control gain K_p dictates how fast the control signal will react to an error between D_{fp} and N_{fp}. It is noted that large changes in the control signal can drive the system across many different dynamical regimes and it is felt therefore that small values of K_p are usually more appropriate. This seems to be in accordance with the results in Reference [25]. A general rule-of-thumb for selecting this gain seems unlikely to be effective because of the great variety of nonlinear systems to which this control scheme could be applied.

The choice of N_t should be based on the time required for the oscillator to reach steady-state. Note that if the output is still under the influence of transients, even if the system is undergoing regular motions, the number of points in P will tend to be equal to N_s thus giving a false indication of the actual dynamics.

Finally, it is emphasized that because the sensor output is an integer number, this procedure is particularly robust to noise. In this respect, the tolerance ϵ plays an important role since ϵ is used to determine how many fixed points are in P. Thus robustness with respect to noise is guaranteed if

$$max\{\text{ noise amplitude }\} \leq \epsilon \tag{9}$$

because, in this case, N_{fp} will remain unchanged compared to the noise-free situation.

If the value of ϵ is too large, the FPCA might count two (or more) fixed points as a single one. Conversely, if ϵ is extremely small the FPCA will invariably return $N_{fp} = N_s$ *if* the robustness condition of equation (9) is not satisfied.

4 Controlling Limit-Cycles and Chaos in the Duffing-Ueda Oscillator

The control scheme proposed in §3 is very simple and robust but cannot be used if it is desired to drive the oscillator to a *specific* orbit. Besides, a main drawback of that procedure in a general application is that if there is no *a priori* knowledge concerning how the dynamics of the system will be affected by the addition of the weak force, it cannot be guaranteed in general that a particular weak force will effectively suppress chaos or even drive the system to a periodic motion with the desired periodicity. Consequently the controller may repeatedly increment the amplitude of the control action up to a point where it would no longer be considered a 'weak' force. In what follows a model-based strategy is suggested which remedies these difficulties.

4.1 Model-based control strategy

Consider the block diagram in Fig. 5. It is initially assumed that a model of the actual oscillator is known. This model can then be used to generate a desired dynamical orbit, $y_d(t)$, (a desired attractor) to be tracked by the system output, $y(t)$. Two different situations can be devised, namely i) the regulating problem, in which $u(t)$ and consequently $y_d(t)$ are fixed and it is desired that $y(t) \approx y_d(t)$ in the presence of unknown disturbances, and ii) the tracking problem, in which $y_d(t)$ is changed via $u(t)$ and it is desired that $y(t)$ tracks $y_d(t)$.

In what follows the following controller was used

$$m(t) = u(t) + K_p [y_d(t) - y(t)] \tag{10}$$

and the nonlinear oscillator was simulated as before.

If the model is an accurate representation of the system, then if the inputs to the model and to the oscillator are similar, that is if $m(t) \approx u(t)$ then $y(t) \approx y_d(t)$. This can be readily verified from the controller equation.

In the simulations below the following discrete model was used

$$
\begin{aligned}
y_d(t) &= 2.1579y_d(t-T) - 1.3203y_d(t-2T) + 0.16239y_d(t-3T) \\
&+ 0.22480 \times 10^{-3}y_d(t-3T)^3 - 0.48196 \times 10^{-2}y_d(t-T)^3 \\
&+ 0.19463 \times 10^{-2}u(t-2T) + 0.34160 \times 10^{-3}u(t-T) \\
&+ 0.35230 \times 10^{-2}y_d(t-T)^2y_d(t-2T) \\
&- 0.12162 \times 10^{-2}y_d(t-T)y_d(t-2T)y_d(t-3T) \qquad (11)
\end{aligned}
$$

which has a sampling period of $T = \pi/60$ s and which is valid over a wide range of parameter values [40]. The derivation of nonlinear models identified directly from the system with no *a priori* knowledge and which are useful for control purposes will be discussed briefly in §4.3.

Figure 6 shows the bifurcation diagram of the model in equation (11). This figure indicates the values of A needed to drive the oscillator to a specific dynamical regime, such as period-one, -two, -four, ..., chaos, period-three, -six, ..., chaos, period-one, etc.

In a regulating problem, since the disturbances affect only the system, $y_d(t)$ will remain the same after the disturbances and consequently the oscillator will be forced to remain on the same attractor. A typical tracking problem, would be to, given the oscillator operating on a certain attractor, drive the system to operate at a quantitatively and possibly qualitatively different dynamical regime. The reference signal $y_d(t)$ can be generated by the model by specifying the value of A corresponding to the desired dynamics according to the bifurcation diagram of Fig. 6.

4.2 Simulation results

The following simulations aim at illustrating the main points of the procedure. In what follows $\omega = 1$ rad/s.

4.2.1 Simulation 4

The objective of this simulation is analogous to the simulations one to three, namely to suppress chaos. The main difference between the control scheme described in §3.1 and the

one described in §4.1 is that in the latter the oscillator can be made to track a particular orbit.

Figure 7 illustrates this. The unperturbed ($k=0.1$) oscillator was originally operating in the chaotic regime corresponding to the Poincaré section of Fig. 2b. This was obtained by setting $A = 11$. This was changed to $A = 14$ at $t = 100\,\mathrm{s}$ and, after the transients had died away, the oscillator tracked the new reference signal which is clearly a period-one orbit. The controller gain was $K_p = 8$.

It is noted that the oscillator was controlled throughout the experiment and that the 'set-point' change began at $t = 100\,\mathrm{s}$ but the reference signal attained the final period-one motion at $t \approx 170\,\mathrm{s}$. The tracking between the oscillator and the desired signal is remarkable.

4.2.2 Simulation 5

In this simulation the application of the control strategy in a typical regulating problem is illustrated.

The unperturbed ($k=0.1$) oscillator was initially operating in the period-one motion obtained by setting $A = 11.7$. At $t = 100\,\mathrm{s}$ the system was disturbed. This was simulated by increasing the value of the parameter k from 0.1 to 0.2. The controller gain was also $K_p = 8$.

Figure 8a shows the desired signal and the oscillator output. These signals can hardly be distinguished even after the disturbance. Figure 8b shows the error $y_d(t) - y(t)$ seen by the controller. This signal also indicates that a fairly tight control was achieved. Figure 8c shows the response of the oscillator when no control was performed. This was obtained by setting $K_p = 0$.

It is interesting to realize that multiplying the signal shown in Fig. 8b by $K_p = 8$ one obtains the second term in the controller equation (10) which can be interpreted as the correction needed to alter the input to the model (which would also be the input to the *unperturbed* oscillator operating in open-loop to produce the desired output) in order to attain the control objective. Thus the signal in Fig. 8b is related to the control effort.

A striking fact is that such a correction is smaller after the disturbance has occurred. A possible explanation for this can be conjectured by noting two things. Firstly, if the

perturbed oscillator ($k = 0.2$) were operating in open-loop, this would be driven into chaos by the input $u(t) = 11.7cos(t)$. Secondly, as it has been noted "... a chaotic motion is highly structured and deterministic. It may be thought of as a combination of a possibly infinite number of unstable periodic motions ... the key to controlling chaos is to cull out only the periodic motion that you desire." (Spano *et al.*) [41], "... a chaotic attractor has a large number of unstable periodic orbits embedded in it. It should therefore serve as a rich source of complex periodic wave forms, if an appropriate dynamical control technique can be implemented to stabilize the system." (Roy *et al.*) [18] and, most importantly, "Chaotic systems exhibit extreme sensitivity to initial conditions. This characteristic is often regarded as an annoyance, yet it provides us with an extremely useful capability without counterpart in nonchaotic systems. In particular, the future state of a chaotic system can be substantially altered by a tiny perturbation." (Shinbrot *et al.*) [21].

Therefore it seems appropriate to infer that because the perturbed oscillator would be in a chaotic regime if no control had been performed (see Fig. 8c), then the control effort required to stabilize the oscillator to a periodic motion is less when compared to the unperturbed oscillator. The exploitation of this potential feature of chaotic systems appears to have been the chief motivation for the method of Reference [24].

4.2.3 Simulation 6

The control scheme of Fig. 5 can also be used to track chaotic signals. This is illustrated in Fig. 9a. The oscillator was initially operating in a period-three motion corresponding to $A = 9$. The controller gain was $K_p = 8$. At $t = 100$s a change in the reference signal occurred which forced the oscillator to track the reference model driven by $u(t) = 11cos(t)$ and from Fig. 6 it is clear that the corresponding motion is chaotic. It should be noted that the Poincaré section of the oscillator for $A = 11$ and that of the model of equation (11) are strikingly similar [40].

Figure 9b shows the error $y_d(t) - y(t)$. An interesting thing to point out is that this error was periodic while the reference signal was periodic, and random (perhaps chaotic) when the reference signal was chaotic. This is illustrated in Figs. 10a–b where 200 cycles have been represented in each pseudo-phase plot.

Finally, the effect of noise is illustrated in Figs. 11a–c which show the tracking error

during experiments similar to the one of Fig. 9.

In the experiment corresponding to Fig. 11a, white noise with variance σ^2=0.021 was added to $y(t)$. Figure 11b illustrates the case where the noise had variance σ^2=0.084. In both cases K_p=8. It is noted that these noise levels are several times higher than typical values considered by other authors [24]. Clearly, an increase in the noise variance produced an increase in the error which, as argued before, is proportional to the control effort. Thus noise with too large a variance will induce large and somewhat random control signals which would eventually prevent tight control. This can be observed in Fig. 11b, where a burst in the error signal occurs between $t \approx 170$ s and $t \approx 330$ s. It is noted that the magnitude of this burst is considerably larger in Fig. 11b than in Fig. 11a.

A way of reducing the effect of noise is to reduce the gain K_p which magnifies the deviations of $y(t)$ from $y_d(t)$. This is illustrated in Fig. 11c where σ^2=0.084 and K_p=2. Note that the magnitude of the bursts in the error signal are considerably smaller and the duration of the bursts is also shorter than before.

The control scheme of Fig. 5 is very simple and effective. Only one parameter, namely K_p, has to be chosen if the controller in equation (10) is used. It is noted that the choice of this parameter is not critical. Large values of K_p usually result in tighter control in noise-free environments. If noise is present, however, the value of K_p should tradeoff tracking capabilities and robustness. This was illustrated in Figs. 11a–c.

4.3 The reference model

The 'Model' in Fig. 5 plays an important role in the model-based control strategy described in §4.1. It is therefore desirable to be able to obtain such a model directly from the original system with no *a priori* knowledge. This problem has been successfully overcome. The identification of NARMAX (nonlinear autoregressive moving average model with exogenous inputs) models is now considered a standard problem in the identification of a large class of nonlinear systems [42, 43, 44, 45, 46, 47, 48, 49]. In particular, the identification of polynomial NARMAX models for the Duffing-Ueda oscillator has recently been reported [50].

An important requirement which must be fulfilled by the nonlinear model of Fig. 5

is that the bifurcation diagrams of the unperturbed system and of the model should be as close as possible. It is stressed that this requirement is usually overlooked in most identification problems where the main objective is usually to obtain models which fit the data records almost in a point-to-point basis at the expense of overparametrization. In such cases an extremely good fit may be obtained but this has been shown to have disastrous effects on the bifurcation structure of the identified models [50].

Therefore, for control purposes in particular, it is crucial that the reference model bifurcates to qualitatively similar dynamical regimes at similar values of A when compared to the original oscillator. The importance of capturing the underlying bifurcation structure when identifying nonlinear models from data records has been illustrated in reference [40].

Comparison of Fig. 6 and Fig. 2b shows that the model of equation (11) is appropriate for control applications at least within the ranges of these bifurcation diagrams.

In the literature, some of the suggested schemes for controlling chaos also require a model [16, 21, 51] but no indication is given concerning how such a model can be obtained in practical situations. On the other hand, other approaches do not require a model but eigenvalues and eigenvectors of linear maps, estimated at each iteration, must be repeatedly computed [20, 22].

Although the identification and validation of NARMAX models for control purposes is now well established and documented, and despite all the benefits gained by the knowledge of a model which reproduces the bifurcation pattern of the actual system, the reference model in Fig. 5 may be dispensed with in many control applications. This can be appreciated by noticing that the model in the control scheme of Fig. 5 is only used to determine an appropriate reference signal.

Consequently, in many applications, there is no need for the reference model as long as a *suitable* reference signal $y_d(t)$ be provided. In regulating problems this is very simple because a complete period of the oscillator output, $y(t)$, can be recorded during normal operation, that is before the disturbance occurs, and used thereafter indefinitely as the desired signal irrespective of disturbances.

In tracking problems a collection of suitable desired output periodic signals can be stored in, say, digital memory and subsequently used as the signal to be tracked by the

oscillator.

It would seem natural to wonder why bother using a faithful reference model to generate the reference signal or even why bother storing such signals for later use if the reference model is not available. Why not use a standard signal generator to produce $y_d(t)$? The next simulation aims at clarifying this relevant point.

4.3.1 Simulation 7

In this experiment the oscillator was initially operating in closed-loop with $A = 5.5$ and K_p=8. At $t = 100$ s the reference signal was changed from the output of the reference model excited with $u(t) = 5.5cos(t)$ to the cosine $y(t) = 2.0cos(t)$. Figure 12a shows the reference signal and the oscillator output and Fig. 12b shows the error between these signals. Figure 12c shows the last 50 seconds of Fig. 12a.

These figures clearly reveal that the quality of the tracking has degraded significantly after $t = 100$ s. The remarkable increase in the error signal can also be interpreted as an increase in the control effort. Although the new reference signal is similar to the former one, the tracking error is considerably greater after $t = 100$ s.

This can be explained by noting that the latter reference signal, that is the cosine, is not a 'genuine' orbit of the oscillator in the sense that it is not reproducible by the system and consequently the effort required to track such a signal is much greater. Besides, the tracking quality is clearly not as good as when the reference signal was a natural orbit of the oscillator. This suggests that the reference signal should be a genuine orbit and highlights the importance of obtaining faithful reference models which can be used to provide such signals.

The fact that in simulations 4 to 6 the reference signal, $y_d(t)$, was always a genuine orbit of the unperturbed oscillator (obtained using the discrete model of equation (11)) also serves as a justification for the high quality control achieved in each case. In this respect, the model in Fig. 5 can be viewed as a filter which yields a genuine reference signal when excited by $u(t)$.

Consider the reference and output signals plotted in Fig. 7. The 'set-point' change began at $t = 100$ when the value of A was changed from 11 to 14. Note that although the period-one motion was not established until $t \approx 170$ s, the tracking error was very small

throughout the experiment. This is because the reference signal switched from a chaotic attractor to a period-one attractor via 'genuine transients' which could be followed easily by the oscillator. If the period-one signal had been imposed directly at $t = 100\,\mathrm{s}$, that is without using the reference model, larger tracking errors would have obviously occurred.

5 Conclusions

This paper has investigated the control of the Duffing-Ueda forced oscillator. Two closed-loop schemes have been proposed. The first procedure aimed at suppressing chaos by adding an external weak force to the driving signal. The sensor used in the loop enabled the controller to decide if the dynamics were chaotic or periodic and, in the latter case the sensor also determined the periodicity of the dynamics. Besides suppressing chaos, it has been shown that, in some cases, this procedure is effective in driving the oscillator to orbits of specified periodicity.

In the second procedure a reference model has been used to generate 'genuine' reference signals to be tracked by the oscillator. It has been shown that this control strategy is effective in tracking and regulating problems alike. It has been argued that although the reference model plays an important role in this control procedure, in many applications such a model may be dispensed with as long as genuine reference signals can be provided. In this respect is has also been shown that the quality of the control and the control effort required are considerably degraded if non-genuine reference signals are used.

The proposed techniques do not make some of the assumptions commonly made in other methods. Moreover, the suggested procedures are simple and, to a certain extent, robust with respect to noise.

Finally, it has been pointed out that although both procedures may be applied without a model, much can be gained if models which reproduce the bifurcation behavior of the system are known. Because in practice such models will usually not be available, the identification of nonlinear dynamic models obtained directly from the system without any kind of *a priori* knowledge has to be considered. Hence a procedure for identifying such models based on the NARMAX (nonlinear autoregressive moving average model with exogenous inputs) model has been indicated along with references for further reading. A

NARMAX model for the Duffing-Ueda oscillator, which had been previously obtained with no *a priori* information, has been successfully used thus illustrating the feasibility of the techniques employed.

ACKNOWLEDGMENTS

The authors are grateful to Prof. Yoshisuke Ueda for kindly indicating some of the cited references.

References

[1] R. Van Buskirk and C. Jeffries. Observation of chaotic dynamics of coupled nonlinear oscillators. *Phys. Rev. A*, 31(5):3332–3357, 1985.

[2] M. Hasler. Electrical circuits with chaotic behavior. *IEEE Proceedings*, 75(8):1009–1021, 1987.

[3] S. Wu. Chua's circuit family. *IEEE Proceedings*, 75(8):1022–1032, 1987.

[4] T. Matsumoto. Chaos in electronic circuits. *IEEE Proceedings*, 75(8):1033–1057, 1987.

[5] T. Lin and L.O. Chua. On chaos of digital filters in the real world. *IEEE Trans. Circuits Syst.*, 38(5):557–558, 1991.

[6] D.C. Hamill, J.H.B. Deane, and D.J. Jefferies. Modeling of chaotic DC-DC converters by iterated nonlinear mappings. *IEEE Trans. Power Electron.*, 7(1):25–36, 1992.

[7] M.J. Ogorzalek. Complex behaviour in digital filters. *Int. J. Bif. Chaos*, 2(1):11–29, 1992.

[8] D.C. Hamill. Learning about chaotic circuits with SPICE. *IEEE Trans. Education*, 36(1):28–35, 1993.

[9] A. Wolf. Quantifying chaos with lyapunov exponents. In A.V. Holden, editor, *Chaos*, pages 273–290. Manchester University Press, Manchester, 1986.

[10] J.P. Eckmann and D. Ruelle. Ergodic theory of chaos and strange attractors. *Rev. Mod. Phys.*, 57(3):617–656, 1985.

[11] L. Glass and M.C. Mackey. *From Clocks to Chaos — The Rhythms of Life.* Princeton University Press, Princeton, 1988.

[12] A. Garfinkel, M.L. Spano, W.L. Ditto, and J.N. Weiss. Controlling cardiac chaos. *Science*, 257:1230–1235, August 1992.

[13] L. Glass, A.L. Goldberger, M. Courtemanche, and A. Shrier. Nonlinear dynamics, chaos and complex cardiac arrythmias. *Proc. R. Soc. Lond. A*, 413:9–26, 1987.

[14] A.L. Goldberger, D.R. Ringney, and B.J. West. Chaos and fractals in human physiology. *Scientific American*, pages 34–41, February 1990.

[15] E.R. Hunt. Stabilizing high-performance orbits in a chaotic system: the diode resonator. *Phys. Rev. Lett.*, 67(15):1953–1955, 1991.

[16] Y. Braiman and I. Goldhirsch. Taming chaotic dynamics with weak periodic perturbations. *Phys. Rev. Lett.*, 66(20):2545–2548, 1991.

[17] J. Singer, Y.Z. Wang, and H.H. Bau. Controlling a chaotic system. *Phys. Rev. Lett.*, 66(9):1123–1125, 1991.

[18] R. Roy, T.W. Murphy, Jr., T.D. Maier, and Z. Gills. Dynamical control of a chaotic laser: experimental stabilization of a globally coupled system. *Phys. Rev. Lett.*, 68(9):1259–1262, 1992.

[19] V. Petrov, V. Gáspár, J. Masere, and K. Showalter. Controlling chaos in the Belousov-Zhabotinsky reaction. *Nature*, 361:240–243, 21 January 1993.

[20] E. Ott, C. Grebogi, and J.A. Yorke. Controlling chaos. *Phys. Rev. Lett.*, 64(11):1196–1199, 1990.

[21] T. Shinbrot, E. Ott, C. Grebogi, and J.A. Yorke. Using chaos to direct trajectories to targets. *Phys. Rev. Lett.*, 65(26):3215–3218, 1990.

[22] W.L. ditto, S.N. Rauseo, and M.L Spano. Experimental control of chaos. *Phys. Rev. Lett.*, 65(26):3211–3214, 1990.

[23] S. Rajasekar and M. Lakshmanan. Controlling of chaos in Bonhoeffer-van der Pol oscillator. *Int. J. Bif. Chaos*, 2(1):201–204, 1992.

[24] S. Sinha, R. Ramaswamy, and J.S. Rao. Adaptive control in nonlinear dynamics. *Physica D*, 43:118–128, 1990.

[25] B.A. Huberman and E. Lumer. Dynamics of adaptive systems. *IEEE Trans. Circuits Syst.*, 37(4):547–550, 1990.

[26] T. Kapitaniak. The loss of chaos in a quasiperiodically-forced nonlinear oscillator. *Int. J. Bif. Chaos*, 1(2):357–362, 1991.

[27] R. Brown, L. Chua, and B. Popp. Is sensitive dependence on initial conditions nature's sensory device? *Int. J. Bif. Chaos*, 2(1):193–199, 1992.

[28] Y. Ueda. Randomly transitional phenomena in the system governed by Duffing's equation. *J. Stat. Phys.*, 20:181–196, 1979.

[29] Y. Ueda. Steady motions exhibited by Duffing's equation: A picture book of regular and chaotic motions. In P.J. Holmes, editor, *New approaches to nonlinear problems in dynamics*, pages 311–322. SIAM, 1980.

[30] Y. Ueda. Random phenomena resulting from nonlinearity in the system described by Duffing's equation. *Int. J. Non-Linear Mech.*, 20(5/6):481–491, 1985.

[31] P.J. Holmes. A nonlinear oscillator with a strange attractor. *Philos. Trans. Royal Soc. London A*, 292:419–448, 1979.

[32] J.J. Stoker. *Nonlinear vibrations in mechanical and electrical systems.* Interscience Publishers, Ltd., London, 1950.

[33] W.J Cunningham. *Introduction to nonlinear analysis.* McGraw Hill Book Company, Inc., London, 1958.

[34] F.C. Moon. *Chaotic Vibrations - an introduction for applied scientists and engineers.* John Willey and Sons, New York, 1987.

[35] T.S. Parker and L.O. Chua. *Practical numerical algorithms for chaotic systems.* Springer Verlag, Berlin, 1989.

[36] M.J. Feigenbaum. Universal behaviour in nonlinear systems. *Physica D*, 7:16–39, 1983.

[37] N.H. Packard, J.P. Crutchfiled, J.D. Farmer, and R.S. Shaw. Geometry from a time series. *Phys. Rev. Lett.*, 45(9):712–716, 1980.

[38] F. Takens. Detecting strange attractors in turbulence. In D.A. Rand and L.S. Young, editors, *Dynamical systems and turbulence. Lecture Notes in Mathematics, vol. 898*, pages 366–381. Springer Verlag, Berlin, 1980.

[39] R. Lima and M. Pettini. Suppression of chaos by resonant parametric perturbatios. *Phys. Rev. A*, 41(2):726–33, 1990.

[40] L.A. Aguirre and S.A. Billings. Validating identified nonlinear models with chaotic dynamics. *(Submitted for publication)*., 1993.

[41] M.L. Spano, W.L. Ditto, and S.N. Rauseo. Exploitation of chaos for active control: an experiment. *J. of Intell. Mater. Syst. and Struct.*, 2:482–493, 1991.

[42] S.A. Billings and I.J. Leontaritis. Identification of nonlinear systems using parametric estimation techniques. In *IEE Conf. Control and its applications*, pages 183–187. Warwick, 1981.

[43] I.J. Leontaritis and S.A. Billings. Input-output parametric models for nonlinear systems part i: deterministic nonlinear systems. *Int. J. Control*, 41(2):303–328, 1985a.

[44] I.J. Leontaritis and S.A. Billings. Input-output parametric models for nonlinear systems part ii: stochastic nonlinear systems. *Int. J. Control*, 41(2):329–344, 1985b.

[45] S.A. Billings and W.S.F. Voon. Correlation based model validity tests for non-linear models. *Int. J. Control*, 44(1):235–244, 1986a.

[46] S.A. Billings, M.J. Korenberg, and S. Chen. Identification of nonlinear output affine systems using an orthogonal least squares algorithm. *Int. J. Systems Sci.*, 19(8):1559–1568, 1988.

[47] M.J. Korenberg, S.A. Billings, Y.P. Liu, and P.J. McIlroy. Orthogonal parameter estimation algorithm for nonlinear stochastic systems. *Int. J. Control*, 48(1):193–210, 1988.

[48] S.A. Billings and S. Chen. Extended model set, global data and threshold model identification of severely nonlinear systems. *Int. J. Control*, 50(5):1897–1923, 1989.

[49] S.A. Billings, S. Chen, and M.J. Korenberg. Identification of mimo nonlinear systems using a forward-regression orthogonal estimator. *Int. J. Control*, 49(6):2157–2189, 1989.

[50] L.A. Aguirre and S.A. Billings. Relationship between the structure and performance of identified nonlinear polynomial models. *(Submitted for publication)*., 1993.

[51] T.B. Fowler. Application of stochastic control techniques to chaotic nonlinear systems. *IEEE Trans. Automat. Contr.*, 34(2):201–205, 1989.

Captions

Fig. 1. Series-resonance circuit with nonlinear inductance.

Fig. 2. (a) Bifurcation diagram and (b) Poincaré section of the oscillator for A=11.

Fig. 3. Closed-loop control configuration.

Fig. 4. Poincaré sections, P, during control, (a) chaos, (b) period-12, (c) period-4 and (d) period-8.

Fig. 5. Model-based control configuration.

Fig. 6. Bifurcation diagram for the discrete model.

Fig. 7. Reference signal, $y_d(t)$, and oscillator output, $y(t)$ for simulation 4.

Fig. 8. (a) Reference signal, $y_d(t)$, and oscillator output, $y(t)$, (b) error $y_d(t)-y(t)$, (c) $y_d(t)$ and $y(t)$ when no control is applied

Fig. 9. (a) Reference signal, $y_d(t)$, and oscillator output, $y(t)$, (b) error $y_d(t)-y(t)$.

Fig. 10. Pseudo-phase plots of the error in Fig. 9b (a) periodic, (b) random (probably chaotic).

Fig. 11. Error signals $y_d(t)-y(t)$ (a) noise variance σ^2=0.021 and controller gain K_p=8, (b) σ^2=0.084 and K_p=8, (c) σ^2=0.084 and K_p=2.

Fig. 12. (a) Reference signal, $y_d(t)$, and oscillator output, $y(t)$, (b) error $y_d(t)-y(t)$, (c) last 50 seconds of (a). The reference signal after t = 100 s is not a 'genuine' orbit.

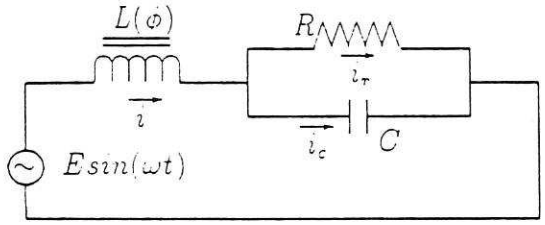

FIG. 1

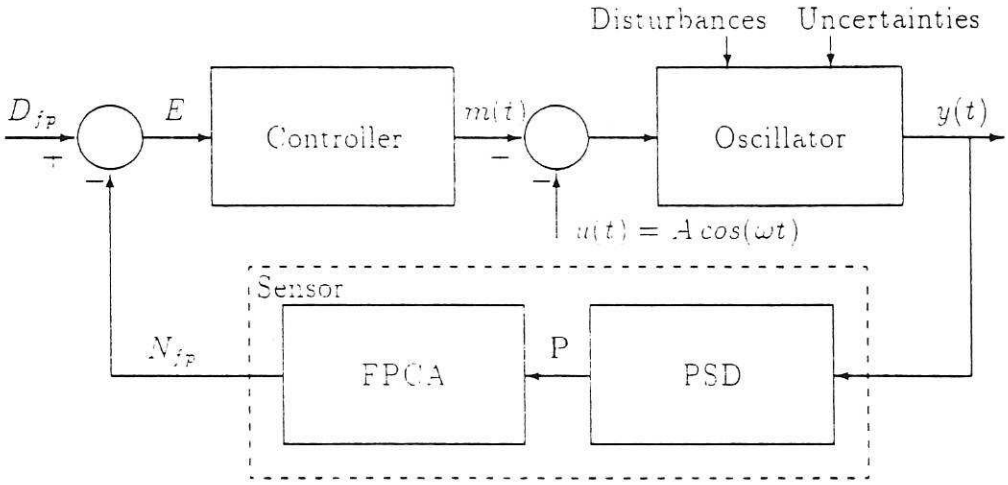

FIG. 3

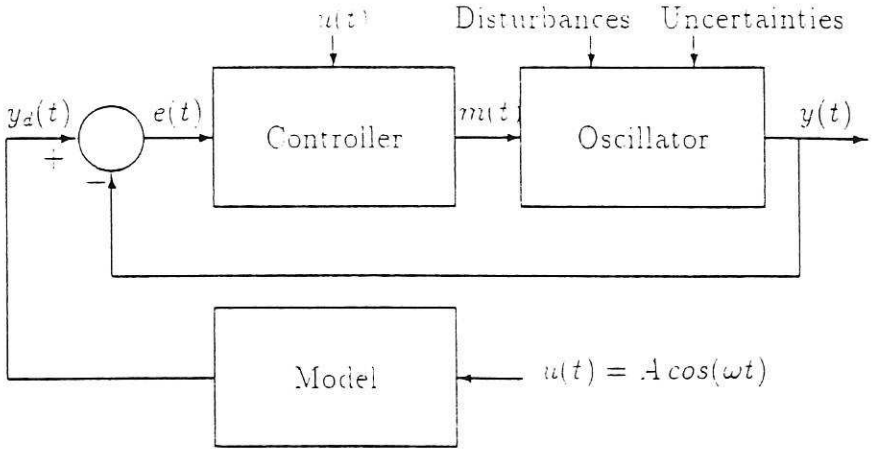

FIG. 5

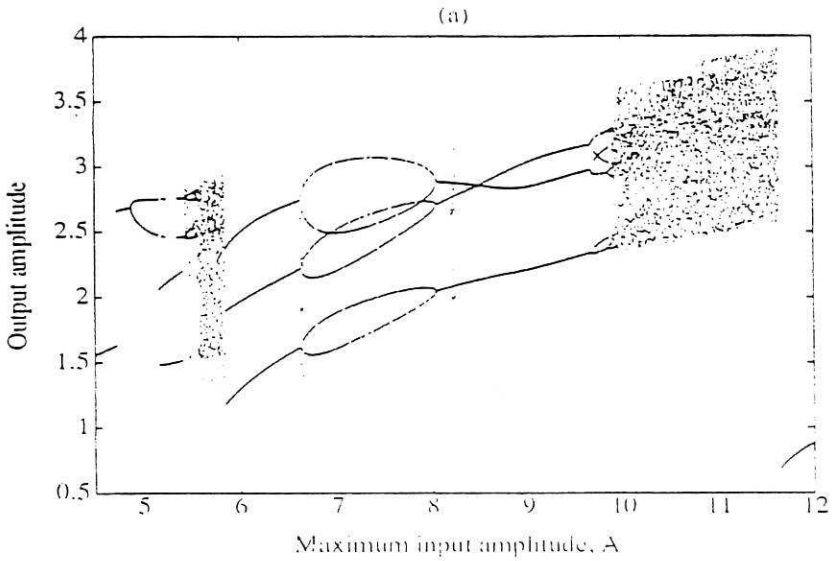
(a)
Output amplitude
Maximum input amplitude, A
4
3.5
3
2.5
2
1.5
1
0.5
5
6
7
8
9
10
11
12

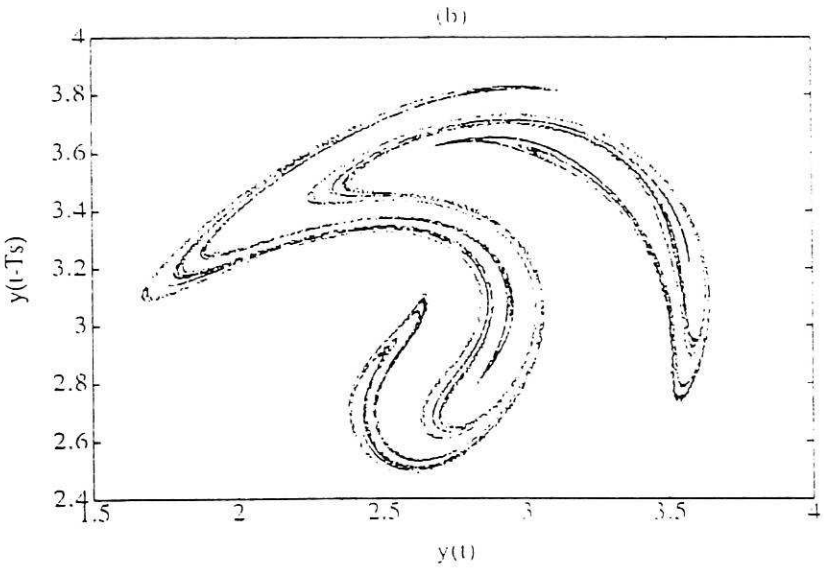
(b)
y(t-Ts)
y(t)
4
3.8
3.6
3.4
3.2
3
2.8
2.6
2.4
1.5
2
2.5
3
3.5
4

FIG. 2

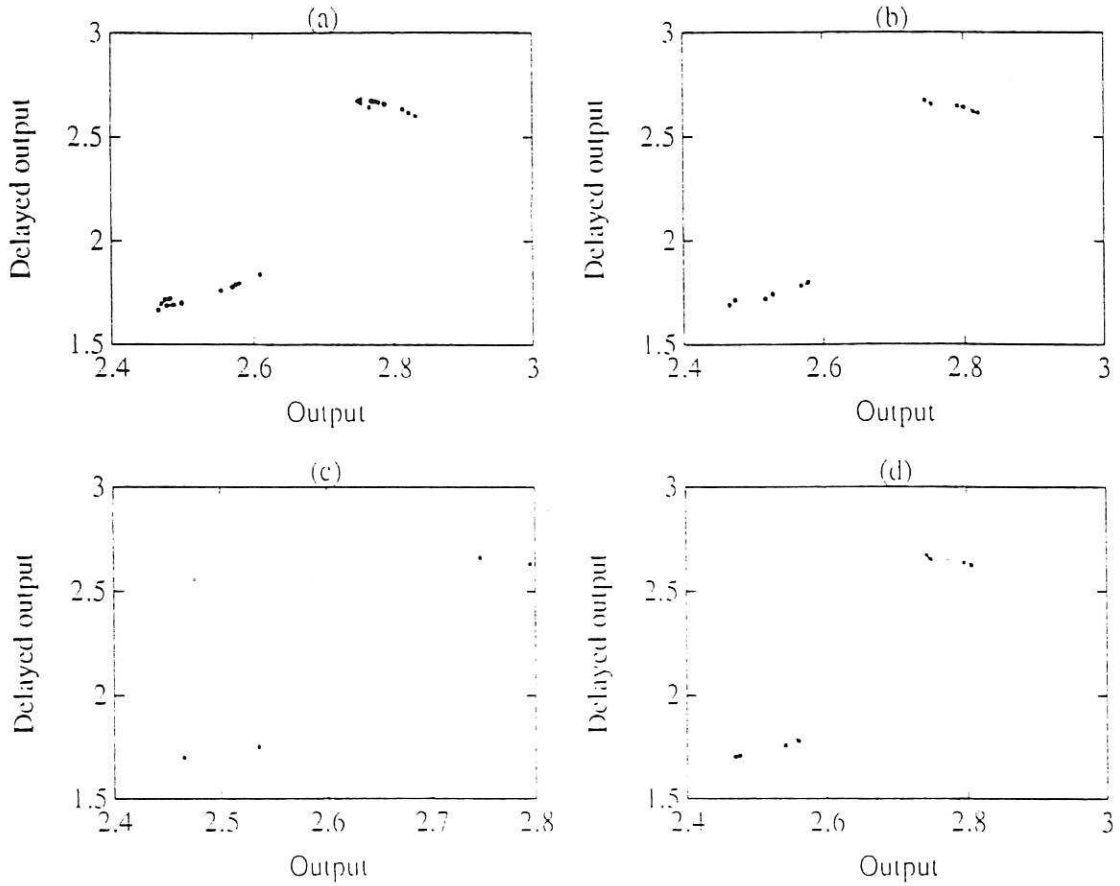
(a)
(b)
(c)
(d)
Delayed output
Output
3
2.5
2
1.5
2.4
2.6
2.8
2.7

FIG. 4

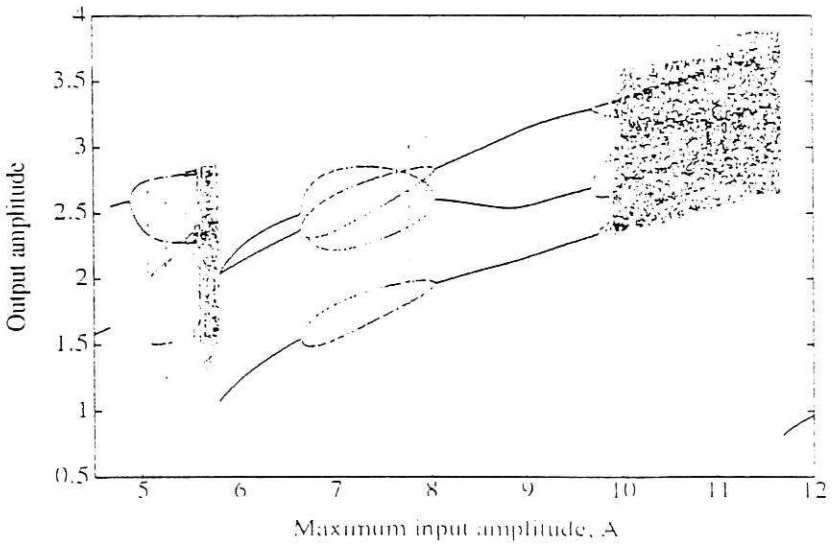
Output amplitude
Maximum input amplitude, A
4
3.5
3
2.5
2
1.5
1
0.5
5
6
7
8
9
10
11
12

FIG. 5

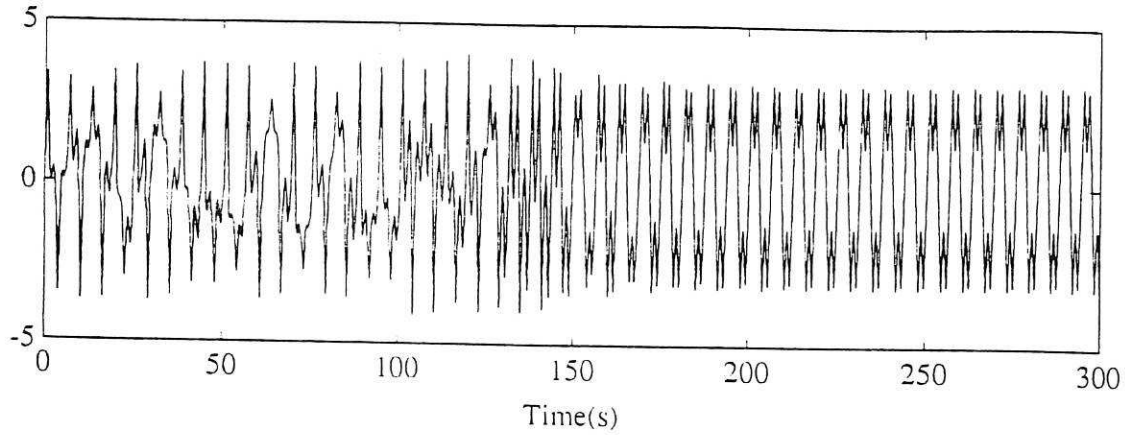

FIG. 7

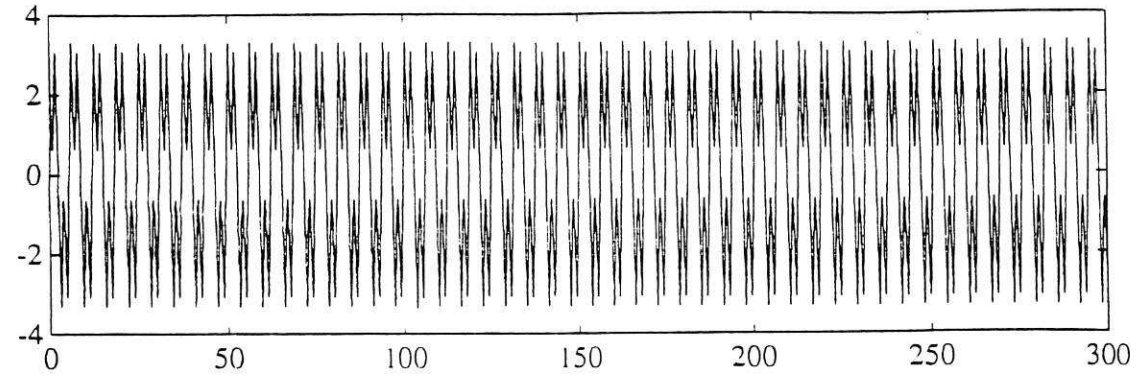

(a) Time (s)

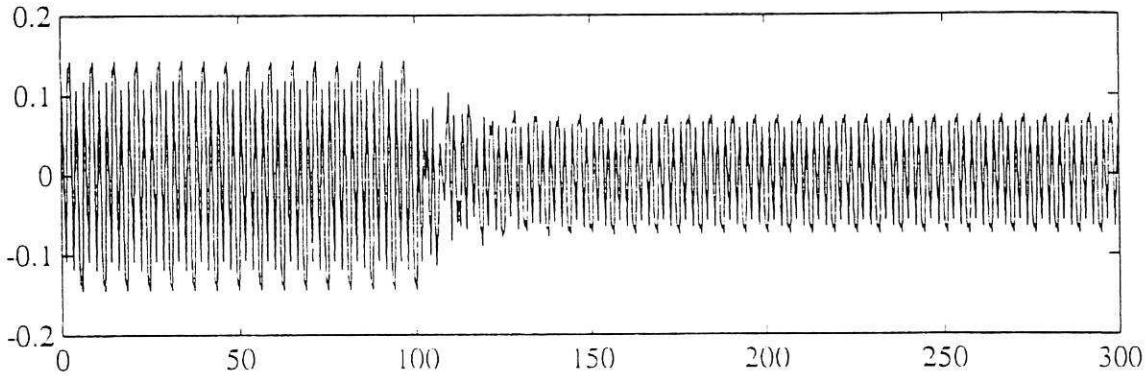

(b) Time (s)

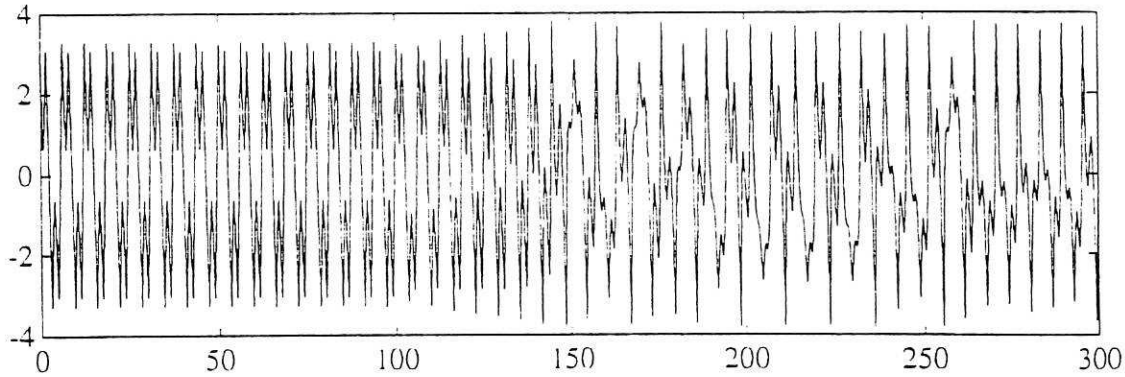

(c) Time (s)

Fig. 8

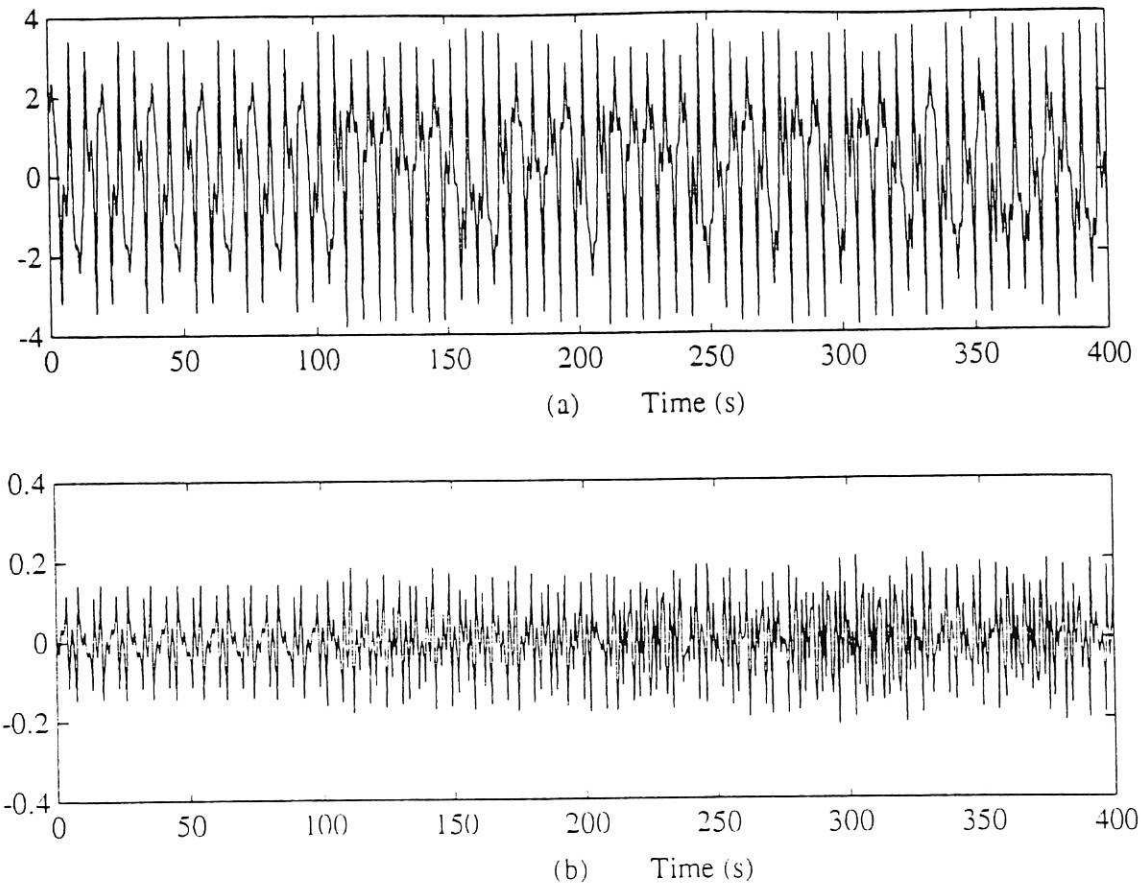
4
2
0
-2
-4
0
50
100
150
200
250
300
350
400
(a) Time (s)
0.4
0.2
0
-0.2
-0.4
0
50
100
150
200
250
300
350
400
(b) Time (s)

FIG 9

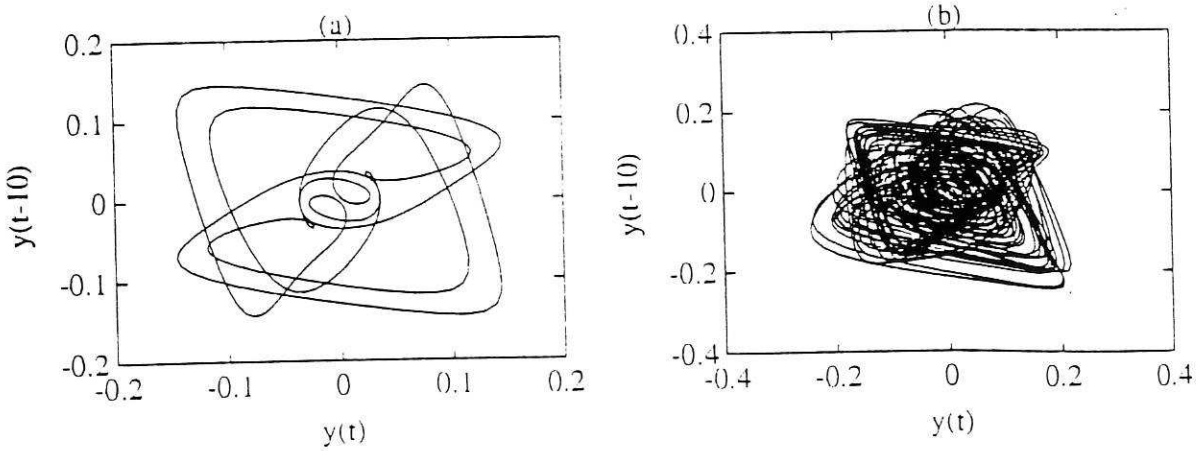
(a)
0.2
0.1
0
-0.1
-0.2
y(t-10)
-0.2
-0.1
0
0.1
0.2
y(t)
(b)
0.4
0.2
0
-0.2
-0.4
y(t-10)
-0.4
-0.2
0
0.2
0.4
y(t)

FIG. 10

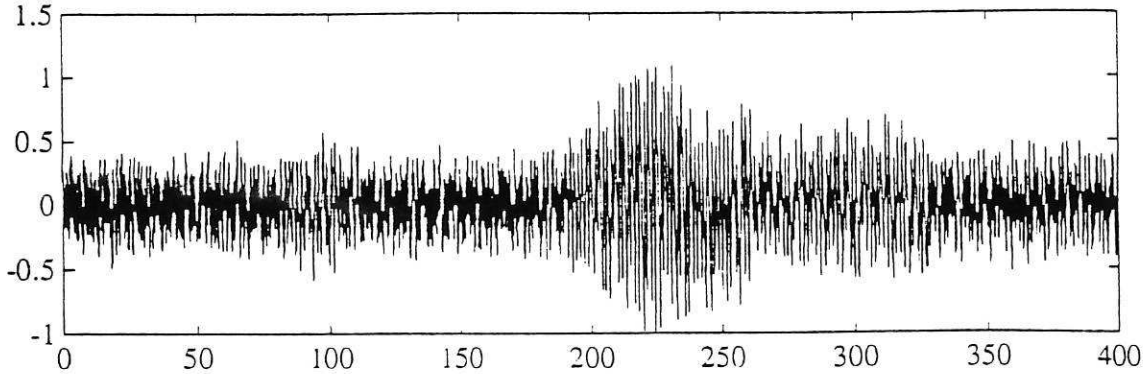

(a) Time (s)

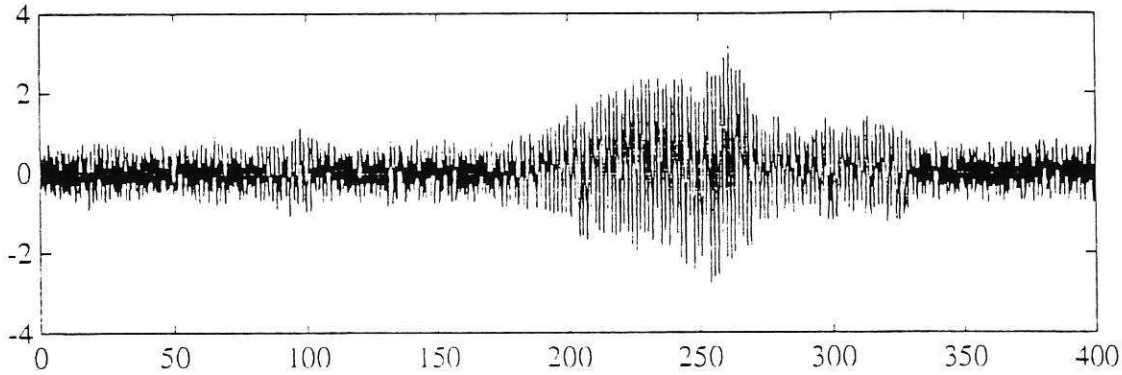

(b) Time (s)

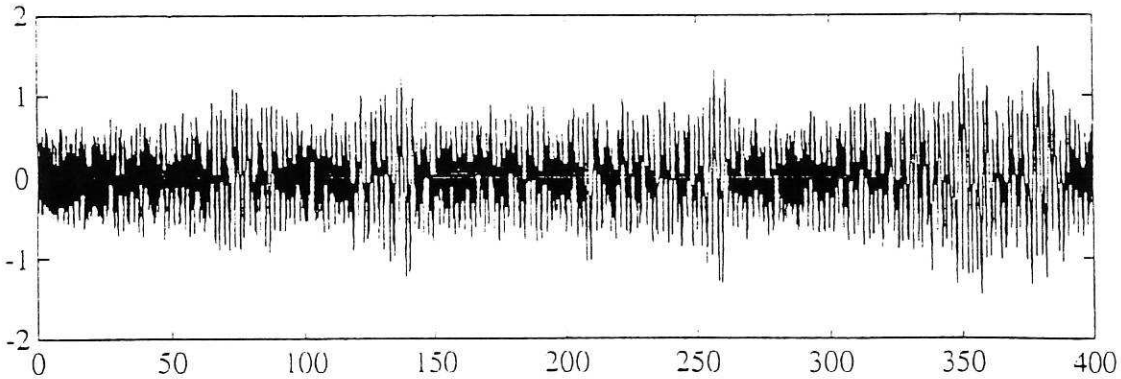

(c) Time (s)

FIG. 11